CYCLIC STRESS ANALYSIS OF AN AIR-COOLED TURBINE VANE

*Albert Kaufman, Daniel J. Gauntner,
and James W. Gauntner*

*Lewis Research Center
Cleveland, Ohio 44135*

1. Report No. NASA TM X-3256	2. Government Accession No.	3. Recipient's Catalog No.
4. Title and Subtitle CYCLIC STRESS ANALYSIS OF AN AIR-COOLED TURBINE VANE		5. Report Date AUGUST 1975
		6. Performing Organization Code
7. Author(s) Albert Kaufman, Daniel J. Gauntner, and James W. Gauntner		8. Performing Organization Report No. E-8237
9. Performing Organization Name and Address Lewis Research Center National Aeronautics and Space Administration Cleveland, Ohio 44135		10. Work Unit No. 505-04
		11. Contract or Grant No.
		13. Type of Report and Period Covered Technical Memorandum
12. Sponsoring Agency Name and Address National Aeronautics and Space Administration Washington, D.C. 20546		
		14. Sponsoring Agency Code

15. Supplementary Notes

16. Abstract

The effects of gas pressure level, coolant temperature, and coolant flow rate on the stress-strain history and life of an air-cooled vane were analyzed using measured and calculated transient metal temperatures and a turbine blade stress analysis program. Predicted failure locations were compared to results from cyclic tests in a static cascade and engine. The results indicated that a high gas pressure was detrimental, a high coolant flow rate somewhat beneficial, and a low coolant temperature the most beneficial to vane life.

17. Key Words (Suggested by Author(s)) Turbine blades Stress analysis Thermal fatigue	18. Distribution Statement Unclassified - unlimited STAR Category 34 (rev.)

19. Security Classif. (of this report) Unclassified	20. Security Classif. (of this page) Unclassified	21. No. of Pages 23	22. Price* $3.25

CYCLIC STRESS ANALYSIS OF AN AIR-COOLED TURBINE VANE

by Albert Kaufman, Daniel J. Gauntner, and James W. Gauntner

Lewis Research Center

SUMMARY

Effects of gas pressure level, coolant temperature, and coolant flow rate on the stress-strain history and life of an air-cooled turbine vane were analyzed. Transient metal temperatures for these analyses were obtained from a transient heat transfer analysis program and from measurements during cyclic tests of the vane in a static cascade facility.

Crack initiation locations were predicted on the basis of cumulative creep damage; locations without tensile strain were ignored. The analysis indicated that increasing the pressure level increased the severity of the fatigue problem at the airfoil leading edge. Lowering the coolant temperature was most beneficial despite larger thermal gradients and more rapid metal temperature transients. Increasing the coolant flow rate resulted in a small improvement in fatigue life.

The cascade tests were conducted by cycling the inlet gas temperature between 922 and 1644 K (1200° and 2500° F) with gas inlet pressures of either 31 or 83 N/cm^2 (45 or 120 psia). The coolant temperatures were 300 to 811 K (80° to 1000° F) and coolant- to gas-flow ratios either 0.035 or 0.075.

INTRODUCTION

Theoretical cyclic-stress analyses were made for an air-cooled turbine vane and compared with experimental results in order to determine the effects of several operational conditions on stress-strain history, vane life and crack initiation locations. Thermal fatigue of turbine blades and vanes has been a life-limiting problem with the earliest gas turbine engines used in aircraft (refs. 1 and 2). With the trend toward higher gas temperatures and pressures and the advent of turbine cooling, the thermal fatigue problem has become more serious because of the higher temperatures and more severe temperature gradients in the cooled turbine hardware.

Although a great amount of research has been conducted on thermal fatigue problems in recent years, most of this research is derived from controlled tests of laboratory

specimens. Published information on thermal transient responses and fatigue lives of turbine blades and vanes under actual engine operating conditions is limited since much of this information is considered to be proprietary by the aircraft engine companies. In reference 3, metal temperature responses and fatigue life predictions were presented for a number of turbine blade and vane cooling configurations under supersonic transport operating conditions. These results were entirely analytical with little explanation given of the life prediction method.

The purposes of this study were to (1) provide metal temperature, stress, and strain histories for a cooled turbine vane under cyclic gas conditions in a static cascade and (2) determine the influence of these conditions on the vane thermal fatigue life (herein defined as the number of cycles to crack initiation) and the crack initiation locations.

Chordwise stress and strain distributions during cycling were calculated by a stress analysis program which was essentially a combination of the steady-state stress relaxation analysis of reference 4 and the cyclic stress analysis of reference 5. Vane thermal fatigue failure locations and relative lives were determined by computing the cumulative creep damage during a cycle and the number of cycles required to use up creep life; this approach was proposed by Spera (ref. 6).

The operational parameters studied were turbine inlet pressure and coolant temperature and flow rate. Analyses were performed for gas temperature cycles from 922 to 1644 K (1200° to 2500° F), gas pressures of 31 and 83 N/cm^2 (45 and 120 psia), coolant temperatures from 300 to 811 K (80° to 1000° F), and coolant- to gas-flow ratios of 0.035 and 0.075.

EXPERIMENTAL APPARATUS AND PROCEDURE

Vane Description

The vane illustrated in figure 1 had an airfoil span of about 10 centimeters (4 in.) and a chord width of about 6.4 centimeters (2.5 in.). This vane was used in both the turbine cooling research engine and the static cascade described in reference 7.

Cooling air was supplied through an inlet tube at the vane tip. The coolant entered a plenum chamber where it was distributed to leading edge and midchord impingement tubes. After impinging on the leading edge, the air circulated around chordwise fins and exhausted through a collector tube at the vane hub. The air impinging on the midchord region section divided so that part discharged through film cooling slots on the suction and vane pressure surfaces and film cooled the trailing edge while the other part flowed through the split trailing edge. The convection cooling effectiveness of the trailing edge was improved by integrally casting pin fins in the split trailing edge.

2

Vane Instrumentation

Two sets of two (2) vanes each were instrumented with Chromel-Alumel thermocouples at the midspan position. In the first set, 10 thermocouples were mounted on each vane at the chordwise locations as shown in figure 2. The thermocouples located at positions 6, 9, and 13 in figure 2 were subsequently added for the second set of test vanes.

The thermocouples were connected to chart recorders and to an IBM 360 computer through a central data recording system. The high speed data acquisition system for recording and reducing the data is discussed in detail in reference 8. Overall accuracy of the thermocouple system was estimated to be within ±0.4 percent of the readings. The instrumentation for measuring gas and coolant temperatures, pressures, and flows are described in reference 7.

Cascade Description

The cascade facility was designed for operation at gas conditions at the test section of 1644 K (2500° F) and 83 N/cm^2 (120 psia) with a supply pressure of 103 N/cm^2 (150 psia). A detailed description of this facility is given in reference 7. The test section was an annular section of a vane row and contained four vanes and five flow channels. The two central vanes were test vanes while the outer vanes completed the flow channels for the test vanes and served as radiation shields. A separate cooling air system was used to supply the test vanes.

Test Procedure

Transient metal temperatures. - The cascade operating procedure was to first set the gas stream temperature at its maximum value of 1644 K (2500° F) and the desired gas pressure and coolant flow rate, temperature, and pressure. After equilibrium was reached, a steady-state recording was made of all the research instrumentation.

The temperature was then reduced to 922 K (1200° F) by reducing the fuel supply to the combustor by means of a solenoid valve. No attempt was made to maintain a constant gas stream flow rate and pressure. The gas total pressure varied 20 percent between low and high temperature conditions. Cooling air was supplied to the vanes from an independent system; therefore, the coolant temperature, pressure, and flow rate were relatively constant. A steady-state recording of the research instrumentation was again taken after equilibrium was attained.

Starting at the low gas temperature condition, an automatic timer-control mechanism was activated. This closed the solenoid valve in the fuel bypass line which in-

creased the fuel flow to the combustor and gave the high temperature gas condition. After 1 minute the control mechanism caused the solenoid to open, resulting in a change from the high to low temperature gas conditions. After another minute, the solenoid was again closed and the cycles repeated.

Cyclic tests were performed at nominal gas pressure levels of 31 and 83 N/cm^2 (45 and 120 psia). Vane metal transient temperatures were obtained during these tests. Effects of coolant temperature level on vane metal temperature were also measured by successively cycling with nominal cooling air temperatures of 300 and 811 K (80° and 1000° F) for the 31-N/cm^2 (45-psia) pressure level. Data for the 83-N/cm^2 (120-psia) pressure level condition were only obtained at a coolant temperature of 589 K (600° F); data at coolant temperatures of 300 and 811 K (80° and 1000° F) were not obtained because of instrumentation difficulties and limits of excessive metal temperatures, respectively.

These tests were conducted by maintaining a coolant- to gas-flow ratio of 0.035 set at the high temperature part of the cycle. In another test, the vane metal transient temperatures were measured at a coolant- to gas-flow ratio of approximately 0.075 set at the high temperature part of the cycle. The test cases and conditions are specified in table I.

Failure locations. - The instrumented vanes and cyclic tests just described for measurement of transient metal temperatures were also used as the basis for determination of failure locations.

The first set of vanes was removed from the cascade after a total of 60 test cycles during which the coolant- to gas-flow ratio was maintained at 0.035 at the high temperature part of the cycle. Cascade testing of the second vane set was terminated upon completion of 20 cycles with a coolant- to gas-flow ratio of 0.075 at the high temperature part of the cycle. All four test vanes were inspected for cracks under a high power microscope and one of the vanes in the first set was sectioned for metallographic inspection.

ANALYTICAL PROCEDURE

Heat Transfer Analysis

Since the stress analysis required more complete metal temperature distributions during the cycle than could be obtained from the experimental data, a theoretical heat transfer analysis was performed for each of the four cyclic cases. Local metal temperatures as a function of time were computed from a heat transfer program consisting of a transient three-dimensional heat transfer solution with a one-dimensional flow network

analysis. Because of inadequate knowledge of the transient gas-side heat transfer coefficients, these were initially assumed and subsequently corrected by an iteration process until there was reasonable agreement between the theoretical and experimental transient and steady-state temperatures.

Case 1 of table I represents the research engine sea-level operating condition. In case 2, a 300 K (80° F) coolant inlet temperature was used to evaluate the effect of coolant temperature on vane metal temperature and life. Case 3 was used to study the pressure level effect. Case 4 duplicated the operating condition of case 1 except for an increased coolant flow rate.

Stress Analysis

The airfoil midspan section was divided into 140 nodal elements. The stress-strain history of each node was calculated by a computer program which was a combination of the stress relaxation analysis of reference 4 and the transient stress analysis of reference 5. This program takes into account the applied loading (in this case, the gas bending load), thermal strains, creep and plastic flow during the transient and steady-state parts of the cycle, and Bauschinger effects. The gas bending moments, which were used as the boundary conditions, were computed by considering the vane to be a beam fixed at one end and guided at the other. Creep and stress rupture properties of the vane material, MAR M302, are presented in table II. These data were obtained from tests conducted on 0.15-centimeter- (0.06-in.-) thick tubular specimens by a NASA contractor. The creep properties were correlated in Larson-Miller form and curve fitted as explained in reference 4. An assumption was made that the creep strains had the same absolute magnitude in both compression and tension for the same temperature, time, and absolute stress value.

Cyclic Creep Damage Analysis

Failure locations and the cycle lives for cases 1 to 4 were determined by computing the creep damage during the fifth cycle. This involved dividing the test cycle into 24 time increments and successively calculating the temperature, stress, accumulated creep strain, and fraction of the creep rupture life used up at each node for each time increment. The sum of the 24 life fractions gave the life fraction for the whole cycle and, consequently, the number of cycles to failure based on the particular cycle analyzed. Only the absolute values of the individual life fractions were used in the summation, that is, compressive creep was treated as giving a positive life fraction. The creep damage computation was based on the fifth cycle by which time the stresses had

5

undergone most of their relaxation due to creep.

In order to account for stress risers due to discontinuities in the vane structure, it would be desirable to apply a strain concentration factor to the strains at nodes adjacent to these discontinuities. Unfortunately, no information was available for determining such a strain concentration factor. Reference 9 recommended the use of a stress concentration factor of 1.4 for film cooling holes based on empirical data. This factor was assumed in the analysis for the computation of life fractions for nodes adjacent to the leading edge chordwise fins and at the pressure and suction side film cooling slots. The problem with using this or any stress concentration factor is that it can result in stresses approaching the ultimate strength and in unrealistically short lives. Therefore, the life predictions are presented herein on a nondimensionalized basis with respect to the shortest calculated life.

RESULTS AND DISCUSSION

Transient Metal Temperatures

The transient metal temperatures based on experiment and heat transfer analyses for cases 1 to 4 are summarized in figures 3 to 6. Some general observations can be drawn from these figures. The vane hot spot location occurred at the upstream side of the pressure surface film cooling slot (location B) during most of the acceleration part of the cycle and at the upstream side of the suction surface film cooling slot (location C) during most of the deceleration, except for case 2. Generally, the cold spot locations were on the inside of the airfoil near the suction-surface film cooling slot (location D) during acceleration and at the inside surfaces of the leading edge on the suction side of the impingement point (location A) during deceleration. Leading edge stagnation point temperatures were higher than the bulk temperatures during most of the acceleration part of the cycle and lower during most of the deceleration part.

The analytical vane temperatures for the design conditions of the static cascade and the research turbojet engine of reference 7, case 1 (fig. 3), are used as a baseline for comparison purposes; this case showed a higher steady-state bulk temperature and slower thermal transient rates than any of the other cyclic cases. The lowest bulk and leading edge temperatures occurred in case 2 (fig. 4) because of the low coolant temperature. However, case 2 also had the most rapid metal temperature transients during the first few seconds of the acceleration and deceleration transients and the largest chordwise temperature gradients. An unusual feature of case 2 was that the hot spot during most of the deceleration was located on the outside surfaces adjacent to the web (locations E and F in fig. 4) unlike the other cases where it normally occurred at the suction side film cooling slot (location C of figs. 3, 5, and 6).

6

The high gas pressure condition (case 3) exhibited rapid metal temperature transients and large chordwise temperature gradients, as shown in figure 5, which were only slightly less severe than in case 2. The high coolant flow rate condition of case 4 (fig. 6) had little effect on the leading edge and the hot and cold spot transients as compared to the baseline case (fig. 3). However, there was a significant reduction in the trailing edge temperature which suggests that the flow in the leading edge and at the film cooling slots was choked and that the additional coolant went to further cool the trailing edge region of this vane.

Strain Cycles

The results of the vane stress analyses are presented for the most critical locations of cases 1 to 4 as nominal strain-temperature response curves with indicated stresses and elapsed times in figures 7 to 10; although stress concentration factors were used in determining the critical locations, only nominal stresses and strains are presented in these figures. Critical locations were in the regions of the leading edge and the film cooling slots.

The largest strain ranges, absolute values of stress, and usually the highest metal temperatures occurred at the upstream sides of the film cooling slots (locations B and C) except for case 1 (fig. 7) where the downstream side of the pressure-surface slot (location B') was critical. Figures 7 to 10 show that the strains at locations B and C were in compression throughout the cycles.

The only case in which crack initiation in the leading edge region appeared to be at the stagnation point (location I) was for the low coolant temperature condition of case 2 (fig. 8). For all the other cases, leading edge failure initiation was predicted for the inside surface on the suction side of the impingement point. The strains during these cycles were predominantly tensile for both locations A and I and were generally much lower in both magnitude and range than for locations B and C. Another critical location in the vicinity of the leading edge was at the inside surface adjacent to the suction-side fins for case 2 (location J in fig. 8); at this position the strain cycles were in both tension and compression. It is noteworthy that many of the cycles in figures 7 to 10 showed the maximum strains occurring during transient conditions rather than at steady state.

Effect of Operational Factors

Predicted nondimensional cyclic lives are presented in table III for the critical leading edge and film cooling slot regions; however, lives at locations where the strain cycles were entirely in compression were disregarded for reasons which will be subse-

quently discussed.

Baseline condition (case 1). - Case 1 is the most severe of the four vane operating conditions from the standpoint of having the shortest expected fatigue life. The shortest time to crack initiation was predicted to occur at the downstream side of the pressure-surface film cooling slot (location B' in fig. 7). This case was the only one of the four cyclic conditions where a fatigue problem was predicted for the film cooling slot regions. Leading edge crack initiation was predicted at the base of the chordwise fins on the suction side of the point of impingement (location A of fig. 7); this was also the predicted critical location for leading edge cracking in cases 3 and 4.

Low coolant temperature condition (case 2). - The improvement in material properties, because of the lower metal temperature, proved more beneficial than the high thermal gradients and more rapid transients proved harmful. This resulted in removing the fatigue problem of the pressure-surface film cooling slot and in increasing the predicted life at the leading edge compared to the baseline condition. The critical location for failure in the leading edge region was on the suction side of the inside surface at the base of the chordwise slots (location J in fig. 8). The lower coolant temperatures gave the best vane design from a life standpoint for the four conditions which were analyzed.

High pressure condition (case 3). - The effect of high pressure level was detrimental to the fatigue life of the leading edge. The calculated leading edge cyclic life for case 3 was the lowest of all four cases. This was despite the fact that case 3 also had a lower coolant temperature than case 1 which would have tended to increase the leading edge fatigue life as shown by case 2. Case 3 showed no fatigue problem at the pressure-side film cooling slot as in case 1.

High coolant flow condition (case 4). - Increasing the coolant- to gas-flow ratio from 0.035 for case 1 to 0.075 for case 4 eliminated early cracking at the pressure-surface film cooling slot and improved the life at the leading edge slightly.

Comparison of Actual and Predicted Locations and Cycles to Failure

The cyclic creep damage analysis predicted that a crack would initiate at the downstream side of the pressure-surface film cooling slot (location B') for case 1. Fatigue cracks downstream of the film cooling slots on the pressure surfaces of a pair of the test vanes (fig. 11) bear out the predicted crack location. These vanes had undergone about 60 cycles at a combination of conditions of cases 1 to 3. There were no signs of cracks near the suction-side film cooling slot. A second set of vanes, which was cycled 20 times at the conditions of case 4, showed no external evidence of cracking. After the stress and life analyses had predicted leading edge crack initiation at location A (figs. 7 and 9) for cases 1 and 3, a vane from the initial set was sectioned for inspection of the

inside surfaces. This inspection revealed extensive cracking at the base of the leading edge chordwise fins (location A) as shown by the photomicrographs of figure 12. The wide crack seen in figure 12(a) actually propagated to the outside surface; other signs of cracking are seen in figure 12(b).

The predictions of crack locations are also in agreement with experimental results from the research turbojet engine of reference 7 which used the same test vane configuration. The vanes were removed after a majority of the vanes completed about 300 hours of operation which included approximately 130 thermal cycles (many of which were similar to case 1). Inspection with a high-powered microscope disclosed that 69 of 72 vanes exhibited fatigue cracks in the region of the pressure-side film cooling slot and incipient cracks in the leading edge coating. Some of the cracked vanes were known to have been replacements which had undergone less than 100 hours of operation.

The nondimensional cycles to failure at the suction-surface film cooling slot shown in table III were lower for cases 2 and 3 than for case 1. If this were actually the case, some indication of cracking should have been seen near these slots in the research vanes. However, such cracks could not be detected, even when the vanes were sectioned. This suggests that cracks cannot be initiated when no tensile strains exist as in the strain cycles for locations B and C in figures 7 to 10. This was the rationale for disregarding locations where the strain cycles were entirely in compression.

SUMMARY OF RESULTS

The effects of gas pressure level, coolant temperature, and coolant flow rate on the stress-strain history and thermal fatigue life of an air-cooled turbine vane were analyzed using measured and calculated transient metal temperatures and a cyclic stress analysis program. The results of this analysis of the thermal fatigue characteristics of an air-cooled turbine vane can be summarized as follows:

1. The design operating condition resulted in the shortest time to vane crack initiation of any of the four operating conditions which were analyzed. Crack initiation was predicted to occur at the pressure surface film cooling slot.

2. Lowering the coolant temperature had the beneficial effect of lowering the metal temperatures and, therefore, improving the material properties; this outweighed the adverse effects of the larger metal temperature gradients and more rapid transients. The lower coolant temperature eliminated the fatigue problem at the pressure-surface film cooling slot and compared to other operational variables was most beneficial to fatigue life.

3. The effect of increasing the pressure level was to make the leading edge more susceptible to fatigue failure than at the other conditions which were studied.

4. Increasing the coolant flow rate also eliminated the critical fatigue problem at the pressure-surface film cooling slot and improved the leading edge life slightly.

5. The predicted locations of failure agreed well with results of the vane operated in a static cascade and a research turbojet engine.

Lewis Research Center,
    National Aeronautics and Space Administration,
        Cleveland, Ohio, March 5, 1975,
            505-04.

REFERENCES

1. Johnston, J. R.; Weeton, J. W.; and Signorelli, R. A.: Engine Operating Conditions That Cause Thermal Fatigue in Turbojet Engine Buckets. NASA MEMO 4-7-59E, 1959.

2. Signorelli, Robert A.; Johnston, James R.; and Weeton, John W.: Thermal-Stress Fatigue Cracking of Turbine Buckets Operating at 1700° F in a Turbine Engine With Frequent Starts and Stops. NASA TN D-125, 1959.

3. Danforth, C.; and Burggraf, F.: Design and Analysis of Cooled Turbine Blades. V - Life Prediction of Selected Designs. (GE-R68AE6105-Pt-5, General Electric Co.; NAS3-7278.), NASA CR-72417, 1968.

4. Kaufman, Albert: Steady-State Stress Relaxation Analysis of Turbine Blade Cooling Designs. NASA TN D-5282, 1969.

5. Stewart, O. L.; and Vogel, W. H.: Methods for Predicting Thermal Stress Cracking in Turbine Stator or Rotor Blades. (PWA-3142, Pratt and Whitney Aircraft; NAS3-7909.), NASA CR-54636, 1967.

6. Spera, David A.: Calculation of Thermal-Fatigue Life Based on Accumulated Creep Damage. NASA TN D-5489, 1969.

7. Calvert, Howard F.; Cochran, Reeves P.; Dengler, Robert P.; Hickel, Robert O.; and Norris, James W.: Turbine Cooling Research Facility. NASA TM X-1927, 1970.

8. Gauntner, Daniel J.; and Kaufman, Albert: Experimental Transient Turbine Vane Temperatures in a Cascade for Gas Stream Temperature Cycling Between 922 and 1644 K (1200° and 2500° F). NASA TM X-3005, 1974.

9. Burggraf, F.; Murtaugh, J. P.; and Wilton, M. E.: Design and Analysis of Cooled Turbine Blades. I - Leading and Trailing Edge Configurations. (GE-R68AE6101-Pt-1, General Electric Co.; NAS3-7278.), NASA CR-54513, 1968.

TABLE I. - RESEARCH VANE CYCLIC CONDITIONS

Case number	Gas temperature range		Coolant temperature		Gas and coolant inlet pressure		Coolant- to gas-flow ratio
	K	°F	K	°F	N/cm²	psia	
1	922 ± 1644	1200 ± 2500	811	1000	31	45	0.035
2	922 ± 1644	1200 ± 2500	300	80	31	45	.035
3	922 ± 1644	1200 ± 2500	589	600	83	120	.035
4	922 ± 1644	1200 ± 2500	811	1000	31	45	.075

TABLE II. - MAR M302 CREEP AND STRESS RUPTURE DATA

Stress, N/cm²	Stress, ksi	Temperature, K	Temperature, °F	Time (hr) to percent creep of -					Rupture life, hr
				0.1	0.2	0.5	1.0	2.0	
24.1×10³	35.0	1033	1400	0.4	1.9	12.5	44	134	367.5
24.1	35.0	↓	↓	1.0	3.4	17.5	57	177	429.5
25.5	37.0			.4	1.3	6.3	18.5	51	291.0
26.2	38.0			.3	1.0	5.5	19	63	210.6
15.2×10³	22.1	1144	1600	0.2	0.8	5.5	21.5	75	456.0
15.2	22.0	↓	↓	.1	.4	4.3	18.5	65	404.1
16.5	24.0			(a)	.2	2.3	10.5	41	220.6
18.6	27.0			(a)	(a)	.5	2.8	11	74.2
19.3	28.0			(a)	(a)	.3	1.5	5.8	58.9
6.2×10³	9.0	1255	1800	3.6	19.5	95	205	-----	307.0
7.6	11.0	↓	↓	1.8	6.2	30.5	63	138	291.0
7.9	11.5			.6	3.7	21.5	57	123	218.5
9.3	13.5			.2	.7	3.4	9.5	23	61.7
10.0	14.5			.1	.6	2.7	7.2	17	44.8
14.5	21.0			(a)	(a)	.1	.3	.7	3.4
3.4×10³	5.0	1311	1900	32	88	215	340	460	510.6
3.9	5.7	↓	↓	5.5	36	127	225	345	385.9
4.5	6.5			1.7	12.7	65	133	193	194.3
5.7	8.2			1.3	4.0	13.5	27.5	48	73.4
6.6	9.5			.6	1.4	4.7	11	21	30.3
7.0	10.2			(a)	.2	1.6	4.8	11.3	32.5

[a]Failure on loading.

TABLE III. - PREDICTED NONDIMENSIONAL CYCLIC

LIVES BASED ON STRESS-TEMPERATURE-TIME

HISTORY FOR FIFTH CYCLE

Case number	Leading edge region	Pressure-surface film cooling slot	Suction-surface film cooling slot
1	37	$^a1$	$^b61$
2	96	$^b21$	$^b14$
3	9	$^b111$	$^b1$
4	48	$^b40$	$^b110$

[a]Cyclic lives nondimensionalized with respect to cyclic life
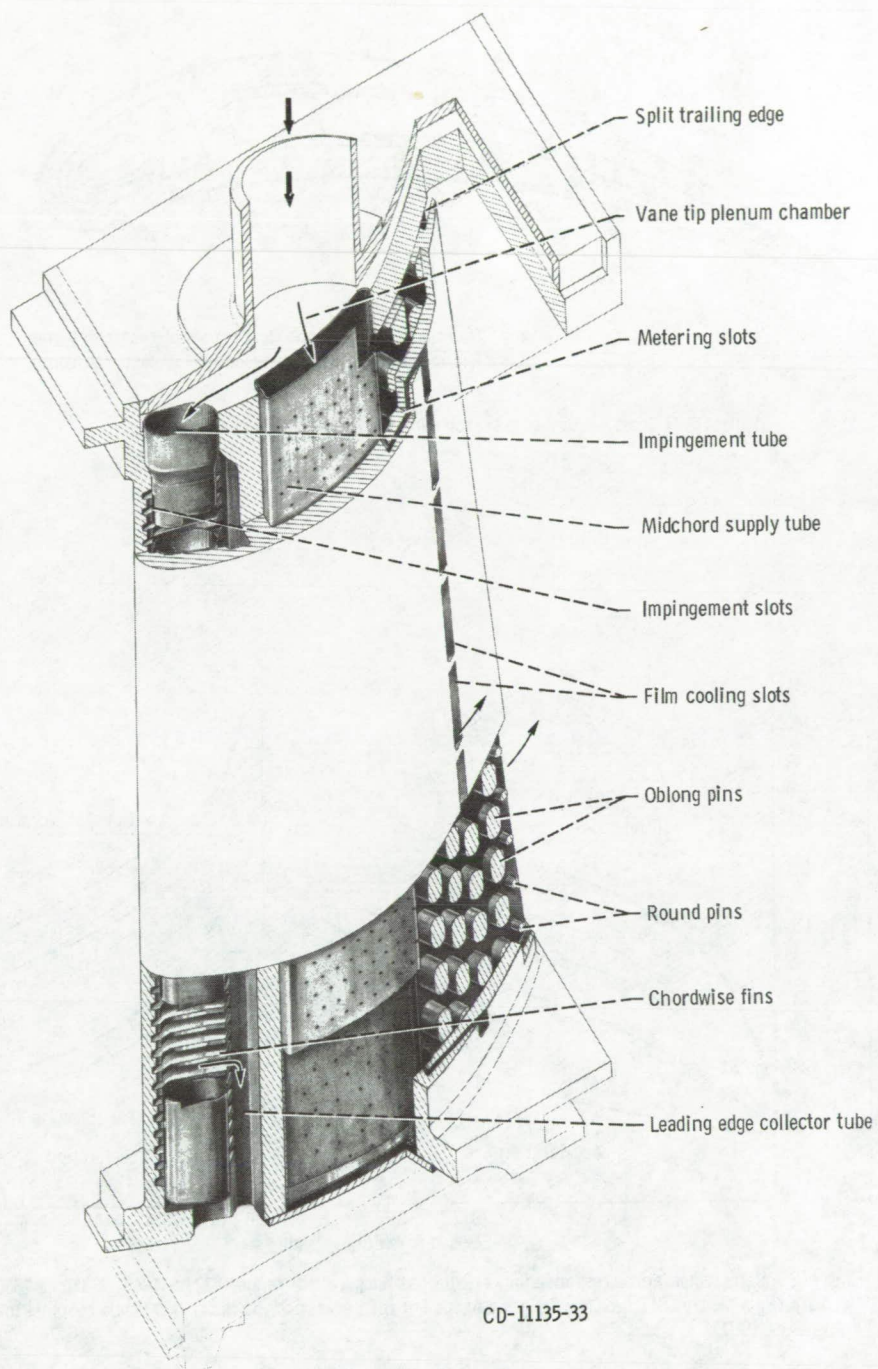 at this failure location.
[b]Strains were in compression throughout cycle.

Split trailing edge

Vane tip plenum chamber

Metering slots

Impingement tube

Midchord supply tube

Impingement slots

Film cooling slots

Oblong pins

Round pins

Chordwise fins

Leading edge collector tube

CD-11135-33

Figure 1. - Research vane.

13
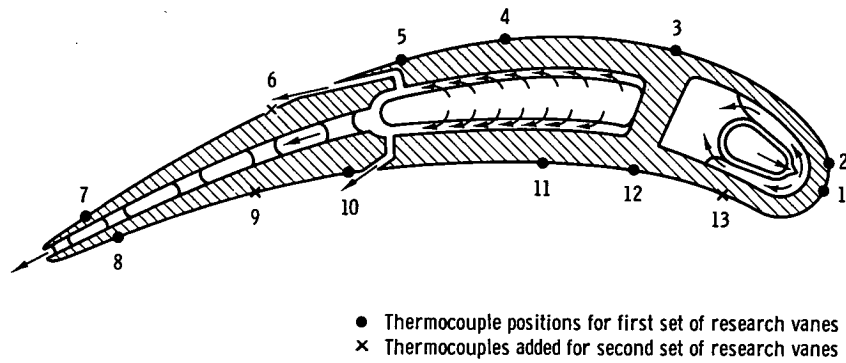
Figure 2. – Cross section of research vane showing thermocouple locations.

● Thermocouple positions for first set of research vanes
✕ Thermocouples added for second set of research vanes
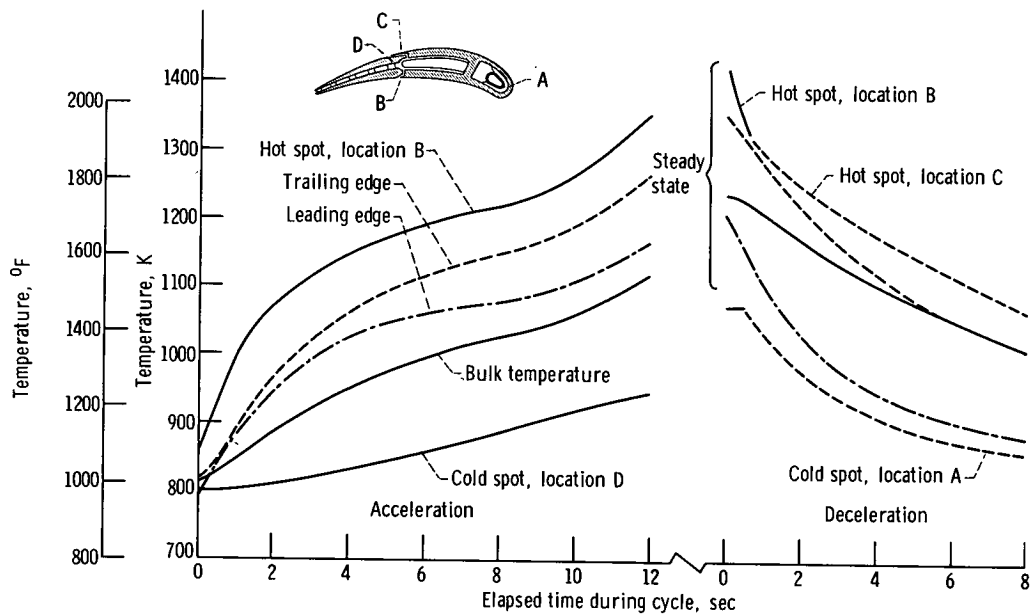
Figure 3. – Vane temperature response for case 1. Gas temperature range, 922 to 1644 K (1200° to 2500° F); coolant temperature, 811 K (1000° F); gas and coolant inlet pressure, 31 N/cm² (45 psia); coolant- to gas-flow ratio, 0.035.
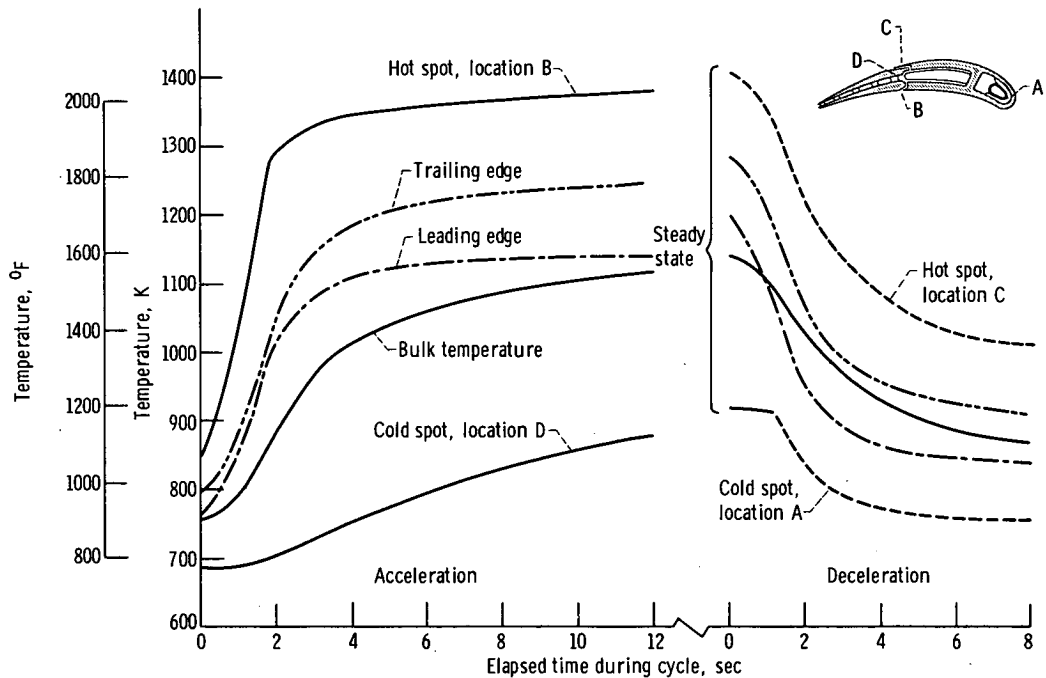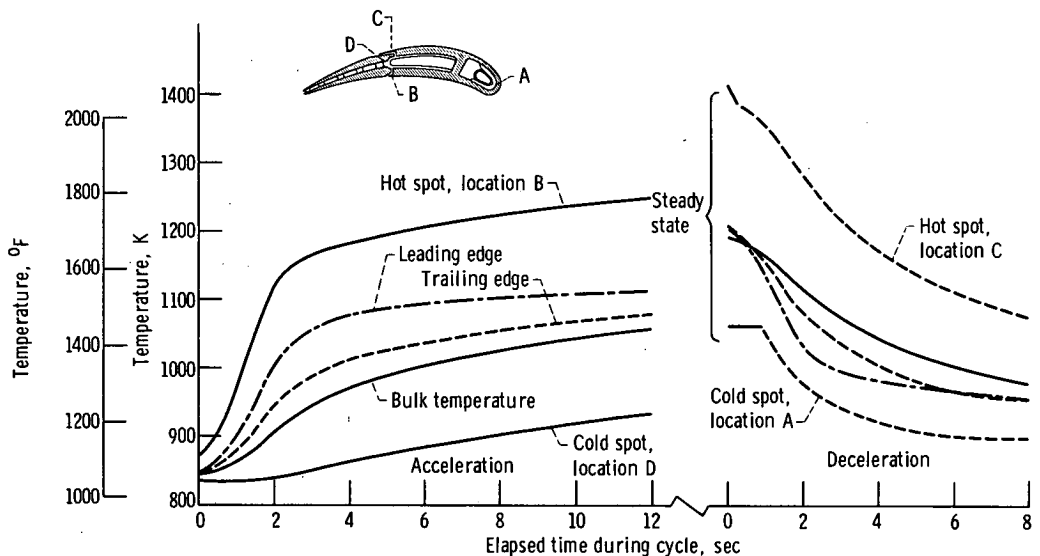
14
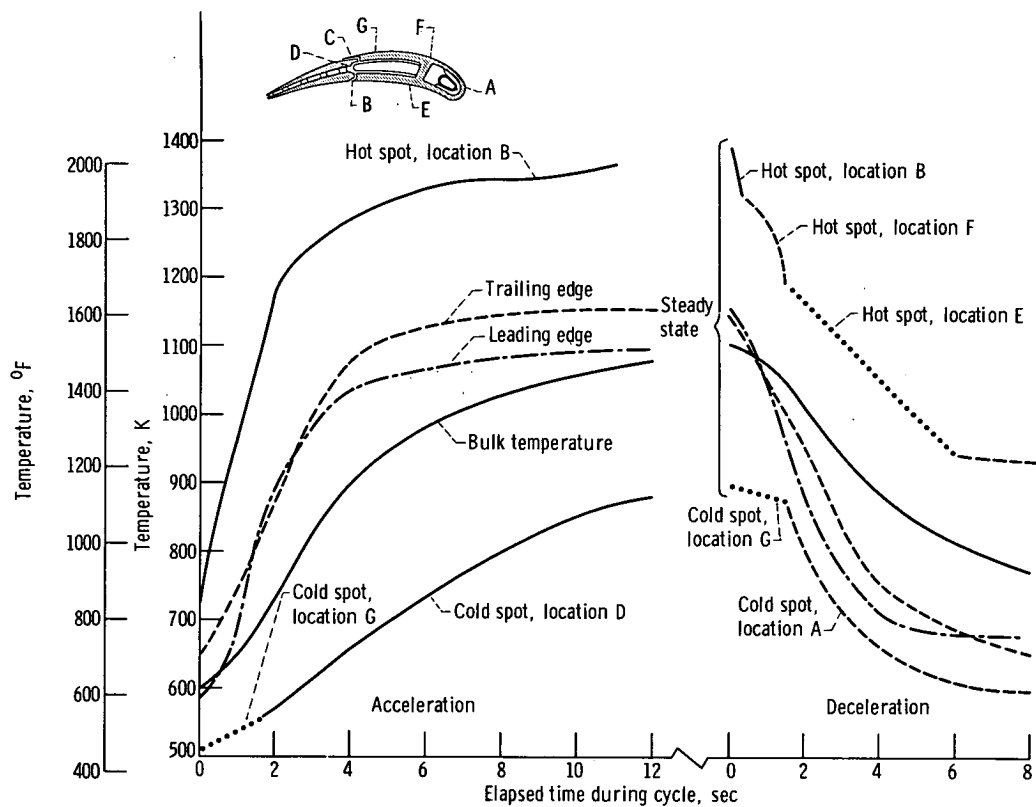
Figure 4. - Vane temperature response for case 2. Gas temperature range, 922 to 1644 K (1200° to 2500° F); coolant temperature, 300 K (80° F); gas and coolant inlet pressure, 31 N/cm² (45 psia); coolant- to gas-flow ratio, 0.035.

Figure 5. - Vane temperature response for case 3. Gas temperature range, 922 to 1644 K (1200° to 2500° F); coolant temperature, 589 K (600° F); gas and coolant inlet pressure, 83 N/cm² (120 psia); coolant- to gas-flow ratio, 0.035.

Figure 6. - Vane temperature response for case 4. Gas temperature range, 922 to 1644 K (1200° to 2500° F); coolant temperature, 811 K (1000° F); gas and coolant inlet pressure, 31 N/cm² (45 psia); coolant- to gas-flow ratio, 0.075.
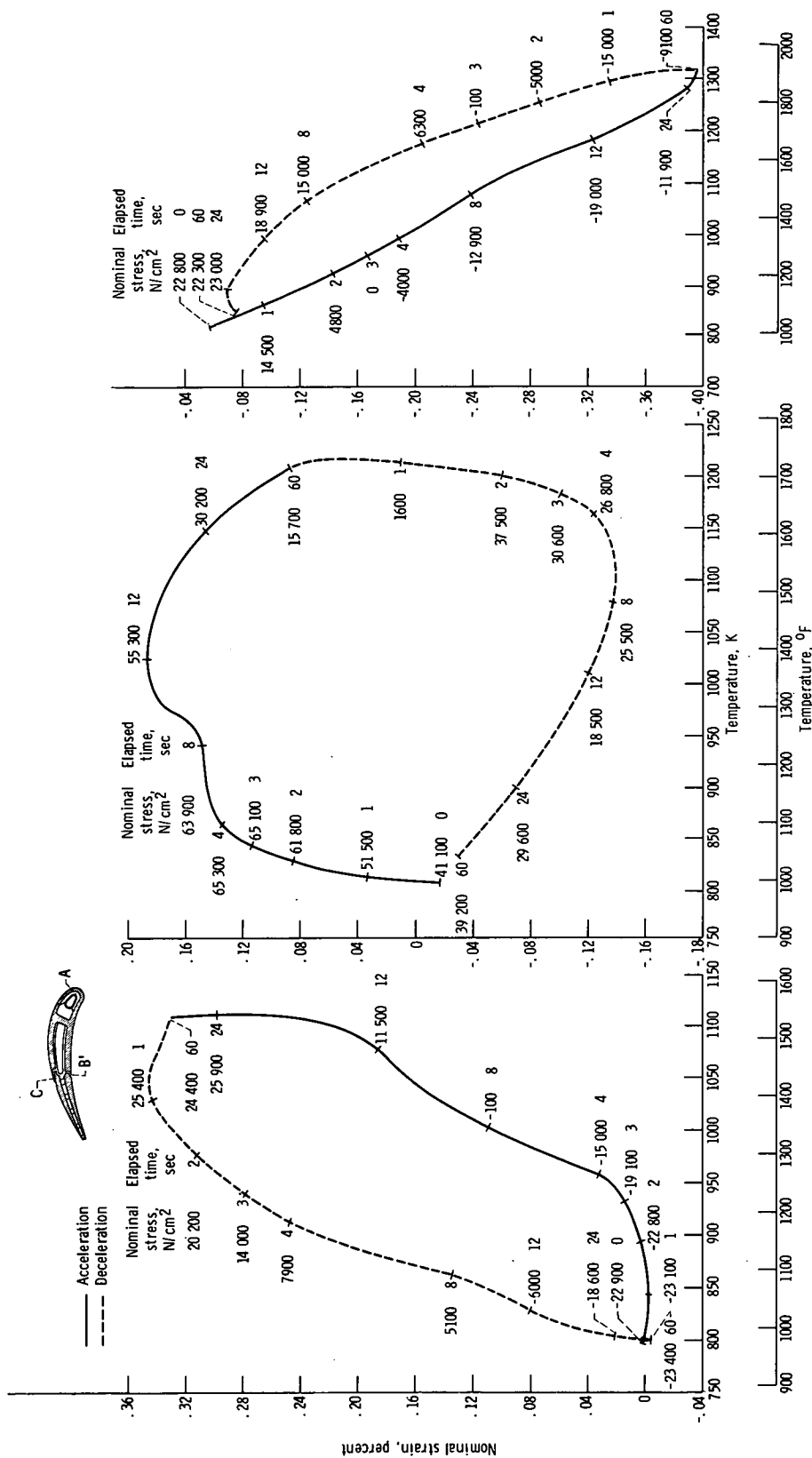
Figure 7. - Strain-temperature response of vane for case 1. Gas temperature range, 922 to 1644 K (1200° to 2500° F); coolant temperature, 811 K (1000° F); coolant- to gas-flow ratio, 0.035; no hold time, fifth cycle.

(a) Critical node at leading edge, location A.

(b) Critical node at pressure side film cooling slot, location B'.

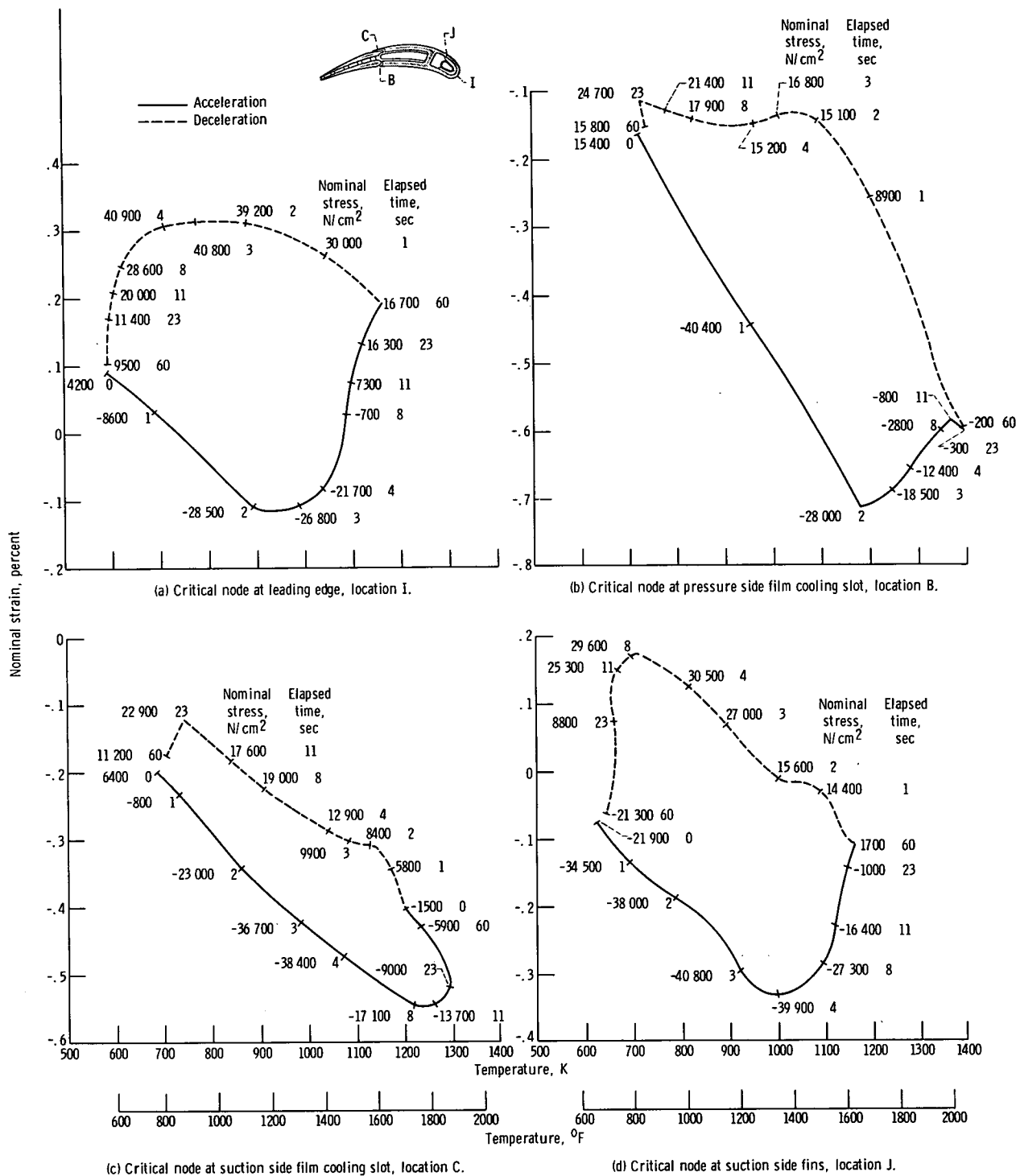(c) Critical node at suction side film cooling slot, location C.

coolant and coolant inlet pressure, 31 N/cm² (45 psia);

17

(a) Critical node at leading edge, location I.

(b) Critical node at pressure side film cooling slot, location B.

(c) Critical node at suction side film cooling slot, location C.

(d) Critical node at suction side fins, location J.

Figure 8. – Strain-temperature response of vane for case 2. Gas temperature range, 922 to 1644 K (1200° to 2500° F); coolant temperature, 300 K (80° F); gas and coolant inlet pressure, 31 N/cm² (45 psia); coolant- to gas-flow ratio, 0.035; no hold time, fifth cycle.
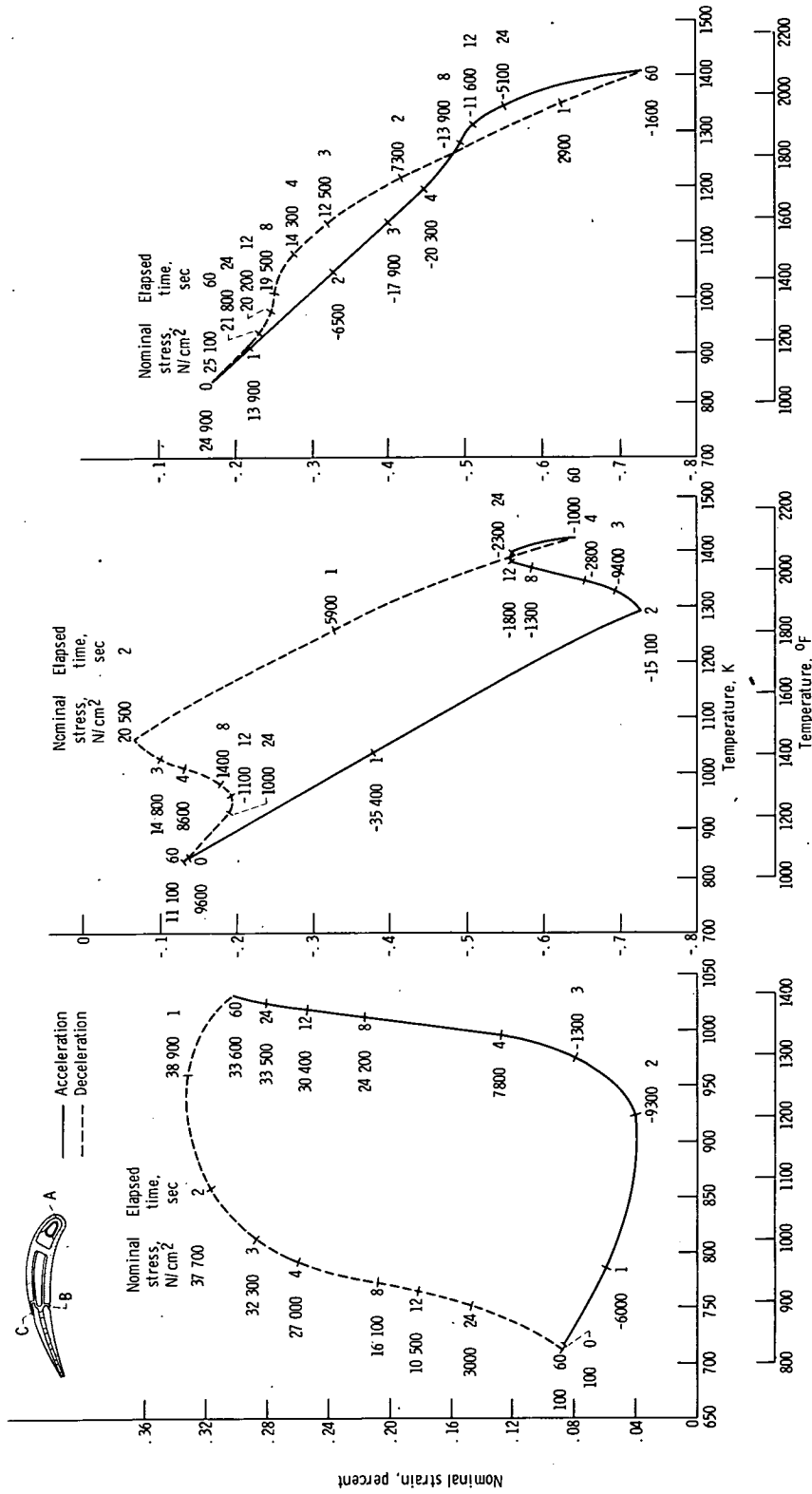
Nominal strain, percent

Acceleration
Deceleration

Nominal Elapsed
stress, time,
N/cm² sec

(a) Critical node at leading edge, location A.

(b) Critical node at pressure side film cooling slot, location B.

(c) Critical node at suction side film cooling slot, location C.

Temperature, K

Temperature, °F

Figure 9. - Strain-temperature response of vane for case 3. Gas temperature range, 922 to 1644 K (1200° to 2500° F); coolant temperature, 589 K (600° F); gas and coolant inlet pressure, 83 N/cm² (120 psia); coolant- to gas-flow ratio, 0.035; no hold time, fifth cycle.
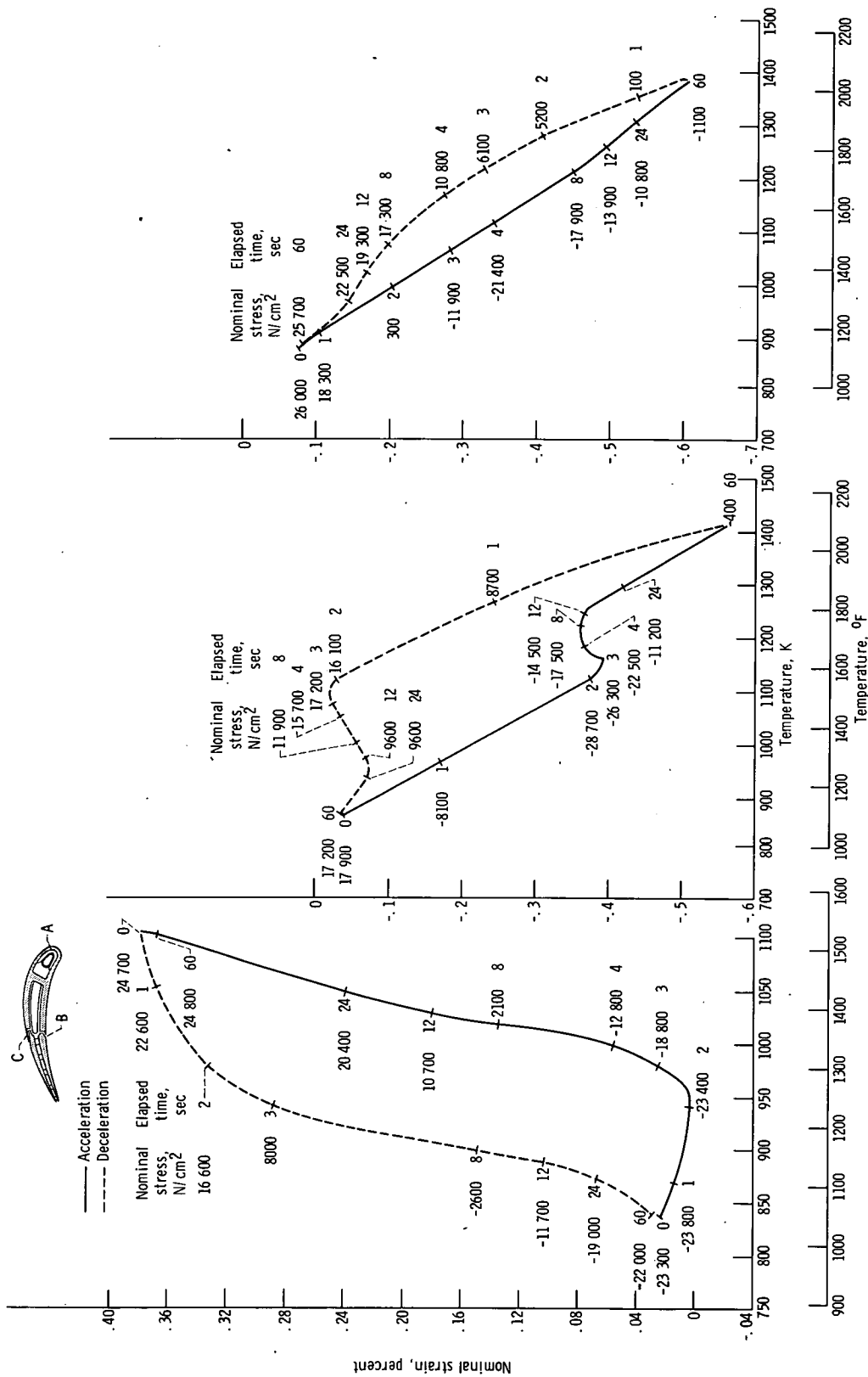
Nominal strain, percent

Acceleration
Deceleration

Nominal stress, N/cm²	Elapsed time, sec

(a) Critical node at leading edge, location A.

(b) Critical node at pressure side film cooling slot, location B.

(c) Critical node at suction side film cooling slot, location C.

Temperature, K

Temperature, °F

Figure 10. – Strain-temperature response of vane for case 4. Gas temperature range, 922 to 1644 K (1200° to 2500° F); coolant temperature, 811 K (1000° F); gas and coolant inlet pressure, 31 N/cm² (45 psia); coolant-to gas-flow ratio, 0.075; no hold time, fifth cycle.
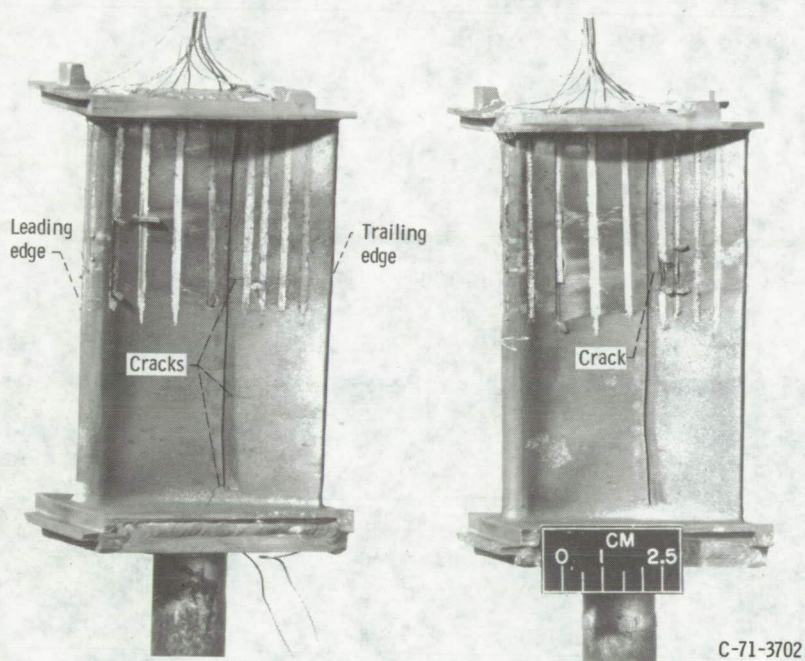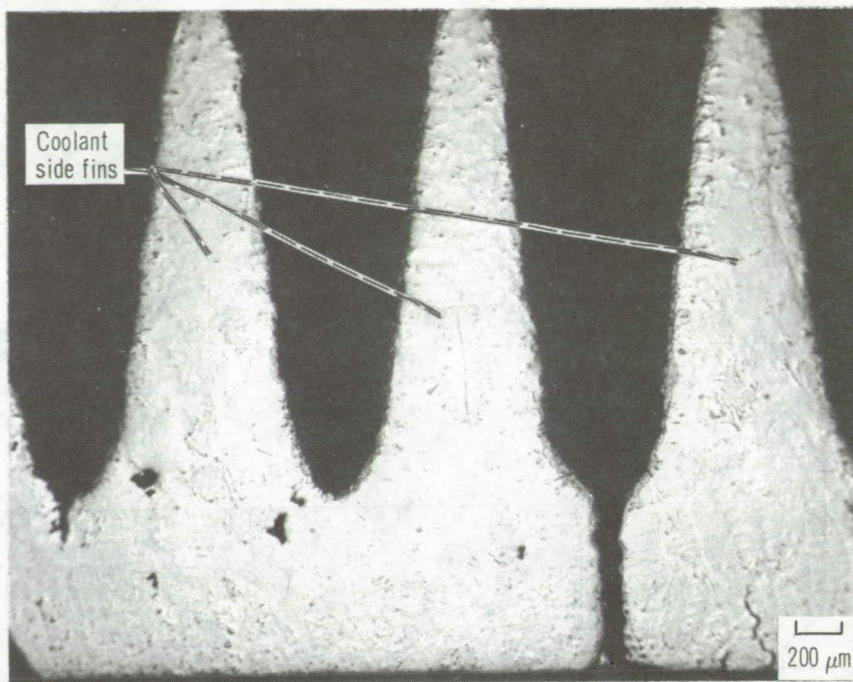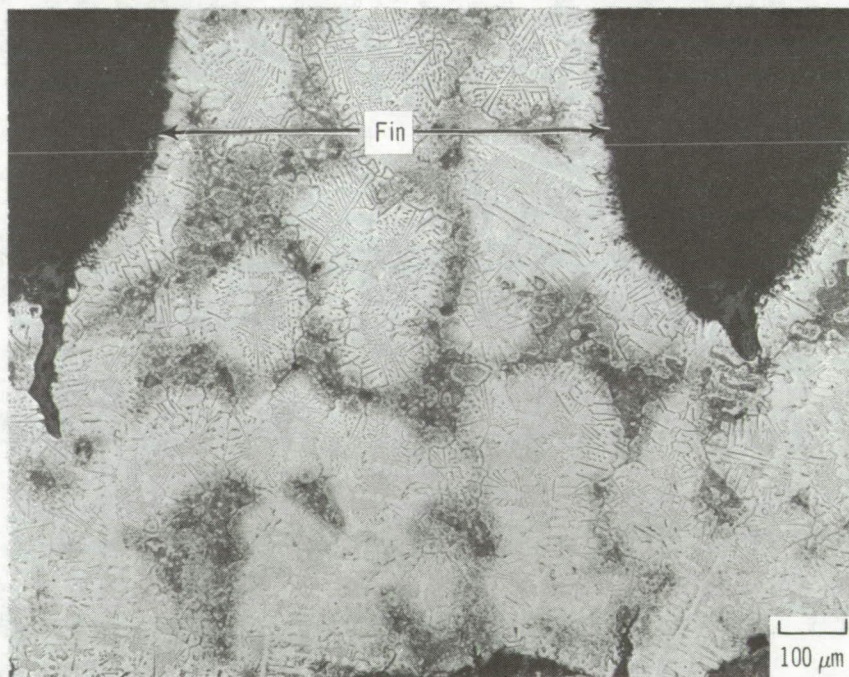
Figure 11. - View of pressure surface of research vanes showing failures near film cooling slot.

(a) Crack propagation through airfoil wall.

(b) Crack initiation at base of fins.

Figure 12. - Fatigue cracks at inside surface of leading edge.

"The aeronautical and space activities of the United States shall be conducted so as to contribute . . . to the expansion of human knowledge of phenomena in the atmosphere and space. The Administration shall provide for the widest practicable and appropriate dissemination of information concerning its activities and the results thereof."
—NATIONAL AERONAUTICS AND SPACE ACT OF 1958

NASA SCIENTIFIC AND TECHNICAL PUBLICATIONS

TECHNICAL REPORTS: Scientific and technical information considered important, complete, and a lasting contribution to existing knowledge.

TECHNICAL NOTES: Information less broad in scope but nevertheless of importance as a contribution to existing knowledge.

TECHNICAL MEMORANDUMS: Information receiving limited distribution because of preliminary data, security classification, or other reasons. Also includes conference proceedings with either limited or unlimited distribution.

CONTRACTOR REPORTS: Scientific and technical information generated under a NASA contract or grant and considered an important contribution to existing knowledge.

TECHNICAL TRANSLATIONS: Information published in a foreign language considered to merit NASA distribution in English.

SPECIAL PUBLICATIONS: Information derived from or of value to NASA activities. Publications include final reports of major projects, monographs, data compilations, handbooks, sourcebooks, and special bibliographies.

TECHNOLOGY UTILIZATION PUBLICATIONS: Information on technology used by NASA that may be of particular interest in commercial and other non-aerospace applications. Publications include Tech Briefs, Technology Utilization Reports and Technology Surveys.

Details on the availability of these publications may be obtained from:

SCIENTIFIC AND TECHNICAL INFORMATION OFFICE

NATIONAL AERONAUTICS AND SPACE ADMINISTRATION
Washington, D.C. 20546